

Journal of Visualized Experiments

Optimized Setup and Protocol for Magnetic Domain Imaging with In-situ Hysteresis Measurement --Manuscript Draft--

Manuscript Number:	JoVE56376R2
Full Title:	Optimized Setup and Protocol for Magnetic Domain Imaging with In-situ Hysteresis Measurement
Article Type:	Invited Methods Article - JoVE Produced Video
Keywords:	Magnetic domain; Bitter method; Steel; BH loop; Dynamic domain imaging; In-situ; Domain wall movement
Manuscript Classifications:	92.26.28: metallography; 92.26.36: physical properties of metals; 97.70.11: magnetism; 97.70.6: electromagnetism; 97.70.8: ferromagnetism
Corresponding Author:	Jun Liu, PhD University of Warwick Coventry, West Midlands UNITED KINGDOM
Corresponding Author Secondary Information:	
Corresponding Author E-Mail:	sam.j.liu@gmail.com
Corresponding Author's Institution:	University of Warwick
Corresponding Author's Secondary Institution:	
First Author:	Jun Liu, PhD
First Author Secondary Information:	
Other Authors:	John Wilson Claire Davis Anthony J Peyton
Order of Authors Secondary Information:	
Abstract:	<p>This paper elaborates the sample preparation protocols, focusing on the extra steps compared to standard metallographic sample preparation procedures, required to obtain optimal domain patterns using the Bitter method. The paper proposes a novel bespoke rig for dynamic domain imaging with in-situ BH (magnetic hysteresis) measurements and elaborates the protocols for the sensor preparation and the use of the rig to ensure accurate BH measurement. The protocols for static and ordinary dynamic domain imaging (without in-situ BH measurements) are also presented. The reported method takes advantage of the convenience and high sensitivity of the traditional Bitter method and enables in-situ BH measurement without interrupting / interfering with the domain wall movement processes. This facilitates establishing a direct and quantitative link between the domain wall movement processes-microstructural feature interactions in ferritic steels with their BH loops. This method is anticipated to become a useful tool for the fundamental study of microstructure-magnetic property relationships in steels and to help interpretation of electromagnetic sensor signals for non-destructive evaluation of steel microstructures.</p>
Author Comments:	Our open access charge fundes requires the compliant RCUK licence, that is Creative Commons Attribution (CC-BY) licence to be signed for.
Additional Information:	
Question	Response
If this article needs to be "in-press" by a certain date, please indicate the date below and explain in your cover letter.	

TITLE:

Optimized Setup and Protocol for Magnetic Domain Imaging with *in situ* Hysteresis Measurement

AUTHORS & AFFILIATIONS:

Jun Liu¹, John Wilson², Claire Davis¹, Anthony Peyton²

¹*Advanced Steel Research Centre, Warwick Manufacturing Group, University of Warwick, Coventry, UK*

²*School of Electric and Electronic Engineering, University of Manchester, Manchester, UK*

sam.j.liu@gmail.com

john.wilson@manchester.ac.uk

Claire.Davis@warwick.ac.uk

a.peyton@manchester.ac.uk

CORRESPONDING AUTHOR:

Jun Liu

j.liu.2@warwick.ac.uk, sam.j.liu@gmail.com

Tel: +44 24765 23783

KEYWORDS:

Magnetic domain, Bitter method, Steel, *BH* loop, Dynamic domain imaging, *in situ*, Domain wall movement

SHORT ABSTRACT:

This paper elaborates the sample and sensor preparation procedures and the protocols for using the test rig particularly for dynamic domain imaging with *in situ BH* measurements in order to achieve optimal domain pattern quality and accurate *BH* measurements.

LONG ABSTRACT:

This paper elaborates the sample preparation protocols required to obtain optimal domain patterns using the Bitter method, focusing on the extra steps compared to standard metallographic sample preparation procedures. The paper proposes a novel bespoke rig for dynamic domain imaging with *in situ BH* (magnetic hysteresis) measurements and elaborates the protocols for the sensor preparation and the use of the rig to ensure accurate *BH* measurement. The protocols for static and ordinary dynamic domain imaging (without *in situ BH* measurements) are also presented. The reported method takes advantage of the convenience and high sensitivity of the traditional Bitter method and enables *in situ BH* measurement without interrupting or interfering with the domain wall movement processes. This facilitates establishing a direct and quantitative link between the domain wall movement processes–microstructural feature interactions in ferritic steels with their *BH* loops. This method is anticipated to become a useful tool for the fundamental study of microstructure–magnetic property relationships in steels and to help interpret the electromagnetic sensor signals for non-destructive evaluation of steel microstructures.

INTRODUCTION:

A variety of electromagnetic (EM) sensors have been developed or commercialized for evaluating and monitoring microstructure, mechanical properties or creep damage in ferritic steels during industrial processing, heat treatment or service exposure ^{1,2}. These sensors operate in a non-destructive and non-contact fashion and are based on the principle that microstructural changes in ferritic steels alter their electrical and magnetic properties. In order to interpret the EM signals in terms of microstructures, one has to link the EM signals to their causal magnetic properties and then to the microstructure of the materials. Relationships between the various EM sensor signals such as mutual inductance for multi-frequency EM sensors and the EM properties (e.g. relative permeability and conductivity) are well established in electromagnetics research with analytical relationships having been reported for several typical sensor geometries³. However, the relationships between the EM or magnetic properties (e.g. the initial permeability, coercivity) and specific microstructures still remain more or less empirical, qualitative or, in many cases, unavailable, particularly when there are more than one type of microstructural features of interest affecting the magnetic behavior ⁴.

Ferromagnetic materials contain magnetic domains, consisting of aligned magnetic moments, separated by domain walls (DWs). As a magnetic field is applied, domains will be re-aligned through DW motion, domain nucleation and growth, and/or domain rotation. More details on domain theory can be found elsewhere ⁵. Microstructural features such as precipitates or grain boundaries can interact with these processes and hence affect the magnetic properties of ferromagnetic materials ^{4,6-8}. The different microstructural features in steels and their magnetic properties can affect the domain structures and the DW movement process when a magnetic field is applied. It is necessary to look into the magnetic domain structure and the interaction between DWs and microstructure features under different applied fields and frequencies in order to establish a fundamental link between the microstructure and magnetic properties in steels.

Magnetic hysteresis loops or *BH* loops can describe the fundamental magnetic properties of the materials such as the coercivity, remanence, differential and incremental permeability, amongst others. *BH* loop analysis has become a useful non-destructive testing (NDT) technique for evaluation of microstructure and mechanical properties of ferritic steels ^{9,10}. The *BH* loop is a plot of the magnetic flux density in the material under inspection (*B*) versus the applied magnetic field (*H*). As a magnetic field is induced in the sample by an excitation coil provided with a time varying current, *B* is measured using a second coil encircling the sample under inspection, while *H* is measured using a magnetic field sensor (commonly a Hall sensor) placed close to the surface of the sample. The most accurate measurement of a material's *BH* characteristics can be made using a closed magnetic circuit, like that presented by a ring sample, but other methods such as the use of a separate excitation core can yield satisfactory results. It is of both great scientific significance and practical value to be able to carry out *in situ* observation of the DW movement processes during magnetic measurements and to directly link these to the magnetic properties and microstructure. Meanwhile, it is very challenging to do either the domain observation or the magnetic measurements without affecting the other.

Amongst various domain imaging techniques, the Bitter method, i.e. using fine magnetic particles to reveal magnetic DWs, has some obvious advantages including easy set-up and high sensitivity¹¹. Due to the use of a medium, e.g. ferro-fluid, it takes a lot of experience and time to obtain high quality patterns and consistent results using Bitter methods. Standard metallographic sample preparation, intended and optimized for optical microscopy (OM) and scanning electron microscopy (SEM), usually yields unsatisfactory Bitter patterns for many steels because the Bitter method is less tolerant to the residual subsurface damage and the associated artificial effects than OM and SEM. There are possible artificial effects due to poor application of ferro-fluid. This paper details additional sample preparation procedures, compared to the standard metallographic ones, preparation and application of ferro-fluid, observation of domain structures using optical microscopes and the method for *in situ* magnetic measurement.

Many studies on the observation of domain structures in single crystals (e.g. Si-iron¹²) or grain-oriented Si electrical steels have been reported¹³. In these materials only a small number of microstructural features (i.e. grain/crystal orientation and grain boundaries) were involved and the domain structures are relatively coarse (with the domain width being on the order of 0.1 mm¹²). In this paper, domain patterns in polycrystalline ferritic steels, including a plain low carbon steel (0.17 wt% C) have been observed and reported. The low carbon steel has much finer grain size (approximately 25 μm on average in equivalent circular diameter) and finer domain structure (with the domain width on the order of micrometers) than the electrical steels and hence show complex interactions between the various microstructural features and DW movement processes.

This paper proposes a novel bespoke rig for dynamic domain imaging using the Bitter method with *in situ* *BH* (magnetic hysteresis) measurements. The reported method takes advantage of the convenience and high sensitivity of the traditional Bitter method and enables *in situ* *BH* measurement without interrupting or interfering with the domain wall movement processes. This facilitates establishing a direct and quantitative link between the domain wall movement processes-microstructural feature interactions in ferritic steels with their *BH* loops. This method is anticipated to become a useful tool for the fundamental study of microstructure-magnetic property relationships in steels and to help interpretation of electromagnetic sensor signals for non-destructive evaluation of steel microstructures.

PROTOCOL:

1 Preparation of specimens for domain imaging with *in situ* *BH* measurement

1.1 Machine two U-shaped parts (Parts A and B) from the steel of interest, as shown in Figure 1, by Electrical Discharge Machining (EDM). Note the difference between the two parts, i.e. 1 mm thicker horizontal part and the 1 mm chamfering in Part A, is designed to ensure a known and needed thickness (1.5 mm in this paper) after the sample (Part A) is mounted and ground (see Figure 1 for the dimensions and procedures 2.1– 2.4 for more details).

2 Preparation of metallographic samples

2.1 Hot-compression mount Part A, preferably using the compounds that produce a

transparent mount.

Caution: Use the correct amount of compounds to avoid damaging the sample during compression mounting. The final thickness of the mount should be 5-10 mm greater than the height of the sample. It is worth noting there might be residual stress caused by the compression mounting, which might then lead to some effects on the domain structure.

2.1.1 Place Part A, with the two legs facing upwards, into the mold of the compression-mounting machine.

2.1.2 Add about 20 mL of methyl methacrylate compound powder into the mold.

2.1.3 Start a mounting cycle with the following parameters: heating time – 4.5 min, cooling time – 4 min, pressure – 290 Bar and temperature – 180 °C.

2.1.4 Take out the mount when the cycle is finished and check the thickness. It should be between 20-25 mm.

2.2 Grind the side of the mounted sample with the two legs of the U-shaped sample facing it using 320 grit SiC paper on a grinding machine until the base of the legs are revealed on the surface. Automated grinding is recommended to ensure the two flat surfaces of the mount are parallel after grinding.

2.3 Grind the other side of the mount and check frequently until the flat part of the U-shaped sample surface shows, grind until the rectangular surface is revealed.

2.4 Measure the length of the revealed sample using a caliper and continue grinding carefully and measure frequently. The revealed sample length will initially increase with grinding (typically slightly over 23 mm when the initial rectangular shape is revealed). Stop grinding as soon as the length reaches 25.05 ± 0.05 mm. At this point, the polished sample will have the same dimensions as the sensor part (Part B in Figure 1) i.e. 25 mm length and 1.5 mm thickness. This procedure, together with the designed chamfering of the sample (Part A Figure 1), gives the known and needed sample thickness, within a tolerance of about tens of microns, after grinding.

2.5 Polish the sample according to the standard metallographic sample preparation procedures for soft steels ¹⁴.

Caution: Do not re-grind the sample, as this will change the sample thickness and therefore cause inaccurate *BH* measurement.

2.6 Etch the polished sample using a cotton swab with suitable reagent (e.g. 2% nital for pure iron or low carbon steel) for 1-5 s until the polished surface turns matte.

2.7 Check the sample under an optical microscope. An effective etching will reveal the microstructure of the sample clearly.

2.8 Polish the sample again using 1 μm diamond polishing agent until the etched surface layer is completely removed. Check under the microscope if not sure.

2.9 Repeat step 2.6-2.8 for 4-6 times. This removes any work hardened surface layer.

2.10 Finish the polishing using alumina suspension for 2 min.

Note: The experiment can be paused here.

3 Preparation of the flux density (B) measurement coil

3.1 Make the sensor using Part B, shown in Figure 1.

3.1.1 Wrap a layer of double sided tape along base of the U shape (i.e. longest side) of Part B.

3.1.2 Using 0.20 mm diameter enameled copper wire, wrap a single layer, 50 turn coil around the longest side of part B, leaving around 100 mm of wire at each end of the coil.

3.1.3 Remove the enamel from the last 20 mm of each end of the wire using 800 grit sandpaper.

3.2 Check for electrical short circuits between coil and sample.

3.2.1 Take a multimeter and set it to test for continuity. Touch one probe to Part B and the other to the end of one wire.

Note: There should be no continuity between coil and sample, if there is continuity between coil and sample, the wire has shorted to the sample and the coil should be removed and re-applied.

4 Set up the domain imaging rig

4.1 Install / fix the samples on the test rig shown in Figure 2.

4.1.1 Place the front plate shown in Figure 2(a) on a flat surface and fit the mounted sample into the hole in the front plate.

4.1.2 Apply hot melt from a glue gun around the circumference of the mounted sample to hold it in place.

4.1.3 Insert Part B through the excitation coils into the bottom of the sample holder; the sample should protrude from the top of the sample holder by around 1 mm.

219 4.1.4 Fix the back plate onto the back of the sample holder and loosely tighten the bottom nuts,
220 ensuring that the Hall sensor is aligned with the sample by visual inspection.

221
222 4.1.5 Apply exciting current to the excitation coil, which forms an electromagnet, for easy
223 assembly and alignment.

224
225 4.1.6 Align the top of Part A with the bottom of Part B, as in Figure 2, with the help of the
226 magnetic force of the aforementioned electromagnet (maximum force felt at perfect alignment)
227 as well as by visual inspection if the sample mount is transparent. Accurate coupling of the Part
228 A and Part B is important to the accuracy of the BH loop measurement. See Discussion for a more
229 detailed explanation.

230
231 4.1.7 Bolt the top plate to the sample holder.

232
233 4.1.8 Tighten the bottom nuts to apply pressure between Part A and Part B. It is worth noting
234 that overtightening may cause stress within the materials and hence stress-induced effects on
235 the domain structure. The test rig should now look like Figure 2(b).

236
237 4.2 Level the sample for a consistently good focusing across the field of vision. This step is
238 highly recommended if an objective lens of 50 times or higher is used and must be done before
239 applying the ferro-fluid.

240
241 4.2.1 Put a piece of modeling clay the size of a cherry onto a clean glass slide.

242
243 4.2.2 Place the test rig on top of the modeling clay with the sample approximately center
244 aligning with the rig.

245
246 4.2.3 Put three sheets of lens tissue on top of the sample surface for protection.

247
248 4.2.4 Level the whole test rig using a levelling press for microscopy with the sample
249 approximately center aligned with the press.

250 251 **5 Magnetic Domain Imaging**

252 5.1 Dilution of oil-based ferro-fluid.

253
254 5.1.1 Draw 1 mL of oil-based ferro-fluid using a pipette and add it to a 5 mL vial.

255
256 5.1.2 Add 0.5 mL of the original solvent (hydrocarbon oil) for the ferro-fluid into the vial.

257
258 5.1.3 Shake for 10 s.

259
260 5.2 Application of ferro-fluid on the sample.

5.2.1 Draw a single drop (about 0.25 mL) of the ferro-fluid using a pipette and apply on the sample surface.

5.2.2 Put a clean microscope slide on the sample and slowly slide the glass slide off the sample surface to form a thin and uniform layer. A good finish should be semi-transparent with an amber color.

5.3 Static domain imaging

5.3.1 Observe the domain pattern under a light microscope before the ferro-fluid dries out. Use ample lighting and a small aperture (by adjusting the aperture diaphragm) for optimal contrast.

Caution: Avoid exposure of the ferro-fluid to strong light longer than necessary as this may dry the ferro-fluid.

5.3.2 Wipe or rinse with acetone to remove the ferro-fluid after domain imaging.

5.3.3 Clean the sample surface thoroughly and dry the sample after experiments.

5.4 Dynamic domain imaging

5.4.1 Attach a high-speed video camera to the microscope.

5.4.2 Apply a magnetic field to the sample to make the DWs move. The present test rig can be used to apply a field of up to 4 kA/m in parallel with the sample surface. A perpendicular field can be applied using a coil with its axis perpendicular to the surface.

5.4.3 Securely fix the sample to the test rig. Apply hot melt around the sample using a glue gun if necessary. The solidified glue can easily be removed after the experiments.

Note: Steps 5.1– 5.2 also apply here.

6 *In situ* BH measurements and domain imaging

6.1 Connect up the *in situ* domain imaging system.

6.1.1 Connect the sensor excitation coils to the power output of the BH analyzer. We used an in-house BH analyzer developed by the University of Manchester. A detailed description can be found in our previous publication¹⁵.

6.1.2 Connect the Hall sensor to the *H* input channel of the BH analyzer.

6.1.3 Connect the sensor *B* coils to the *B* input channel of the BH analyzer.

6.1.4 Connect the *H* and *B* outputs of the *BH* analyzer to two analogue input channels of the Midas DA BNC Breakout box (referred to as DA box hereafter) respectively ensuring that both inputs are set to the ground source (GS).

6.1.5 Connect the Sync In of the high-speed camera to the Sync Out of the DA box.

6.1.6 Connect the Trigger of the high-speed camera to the Trigger of the DA box.

6.2 Input the test parameters in the *BH* analyzer software. The cross sectional area of the sample should be entered in m²; in this case 6×10^6 m².

6.3 Set the data sync parameters as per the instruction of the DA software.

6.3.1 Set the sync out rate (2000 per second) to be the frame rate (500 frame per second) of the high-speed camera multiplied by the number of data points per frame (4 per frame).

6.3.2 Set the pre-trigger length (in percentage) to be same as that of the camera.

6.4 Set the high-speed video camera ready for recording. That is, the camera will start waiting to be triggered.

6.5 Turn on the *BH* analyzer and apply a 1 Hz excitation sinusoidal current to measure the major loop; an image of the *BH* loop will be displayed.

6.6 Check that the measured *BH* loop is roughly as expected in terms of coercive field, remanence, magnetic saturation, etc. If it is not, the mechanical coupling between Part A and Part B should be inspected.

6.7 Trigger the camera either by sending a trigger signal from the *BH* analyzer or by clicking on the Trigger button on DA software interface.

6.8 Stop recording data and video after at least one *BH* loop cycle in the DA software.

6.9 Turn off the *BH* analyzer.

Caution: Do not keep the electric current running through the sample for a long time especially if a direct current (DC) is used, as the current will heat up the sample and quickly dry the ferro-fluid.

6.10 Clean the sample and refresh for future analysis.

REPRESENTATIVE RESULTS:

Figure 3 shows two examples of high quality static domain patterns without any applied magnetic field for an industrial-grade pure iron and a low carbon steel respectively. One can see the DWs

clearly in both materials and different types of patterns including e.g. packets of parallel (or 180°) and 90° DWs, in different grains. Owing to the good quality of polishing, there are no signs of random distortion of domain patterns due to subsurface damage caused by grinding; and the results show a strong link to the microstructure. For example, the 180° DW spacing (typically about 10 µm for pure iron and about 5 µm for the low carbon steel) increases with the grain size (approximately 200 µm for pure iron and 25 µm for the low carbon steel in mean equivalent circular diameter) and the domain patterns are dependent on the grain crystallographic orientation. It should be noted that the DW thickness as observed in Bitter patterns does not reflect the real Bloch DW thickness, which is estimated to be approximately 30 nm for pure iron⁵. The high uniformity of the pattern quality indicates that the application of the ferro-fluid was optimal.

Figure 4 illustrates a few examples of unsatisfactory results due to poor surface preparation, Figure 4 (a) and (b), or if one fails to fix the sample securely during dynamic imaging or to level the sample. Note even a very small offset movement is obvious under the microscope. The video will go out of focus under the action of the applied field perpendicular to the sample surface as illustrated in Figure 4 (c); or the sample will oscillate laterally at the frequency of the applied field in the case of a parallel AC field being applied.

Figure 5 shows a series of domain images extracted from the DW movement process video at different points of the *in situ* measured *BH* loop. The video clearly shows a strong link between the DW movement processes and the position on the *BH* loop. For example, the transition of 180° DWs into 90° ones in region A occur near the 'knee' of the *BH* loop, i.e. between points 1 and 5 during magnetization; and the process reverses between points 225 and 250 during demagnetization, which indicates the domains rotating towards the applied field direction. It is interesting that the majority of 180° DWs in the bottom series of images do not move significantly. The reason for this is unclear. One possibility may be that the applied field direction, which happens to be approximately perpendicular to domain directions and therefore can neither cause the 180° DWs to move nor rotate the domains to align with the field direction. However, the segments marked in region B bulge leftwards and rightwards during magnetization and demagnetization respectively whilst in region C bulges only slightly leftwards. These phenomena seem to indicate there may be subsurface particles or inclusions disrupting the local domain directions to have component parallel with the applied field and hence move under its action. It is also indicative that the magnetization is not fully saturated. Further analysis of the domain direction and microstructural characterization of crystallographic orientation of the grain and of any subsurface particles are needed.

Figure 1 Drawings of the sensor and specimen parts for *in situ* domain imaging (unit: mm).

Figure 2 Schematic assembly drawing of the *in situ* domain imaging rig 4 (a) separate parts before being assembled (b) finished assembly.

Figure 3 Static domain patterns for pure iron and a 0.2 wt% carbon steel.

Figure 4 **Examples of unsatisfactory domain patterns resulting from failing to follow the protocols properly**

(a) disordered domain pattern (same low carbon steel sample as the one in Figure 3) lacking links to microstructure due to poor sample surface preparation; (b) obscure pattern with poor contrast due to poor application of the ferro-fluid on an as-cast extra-low carbon steel sample; (c) domain patterns going out of focus under the action of the perpendicular field of a pure iron sample

Figure 5 **A series of domain images extracted from the domain wall movement process video at frames corresponding to a series of points on the *in situ* measured *BH* loop with marked regions of interest showing domain rotation and likely interactions with microstructural features of an as-cast extra-low carbon steel sample.**

DISCUSSION:

The metallographic sample preparation is critical to the domain pattern quality by the Bitter method. The subsurface damage inherited from initial coarse grinding can obscure the real domain structure. These artificial effects usually result in poor contrast of DWs and many minor domain features associated with the strain due to the damage and sometimes a maze-like pattern. An amorphous surface layer may form due to serious surface damage, which will then give an unrepresentative domain structure. It is therefore important to take great care during grinding metallographic samples for domain imaging to minimize the subsurface damage in the first place. Additional procedures such as the etch-polishing cycles recommended in this paper or a long chemical mechanical polishing are often necessary to remove the remaining damaged surface layer. One needs to take extra care for sample preparation for the *in situ BH* measurement as excessive grinding or re-grinding will change the sample thickness; accurate thickness knowledge is required to determine the correct *B* values, as the flux density in Part A is inferred by the measurement of flux density in Part B. The *B* values outputted by the software are directly proportional to the cross-sectional area provided, so a 10% error in thickness will lead to roughly a 10% error in *B* values; the relationship is however non-linear, so a simple calibration after measurement is not possible. Over-ground samples can still be used for domain imaging but it should be noted that the measured *BH* loops will not be quantitatively representative of the real *BH* curve for the part of the sample being inspected. The *H* measurements should still be approximately representative of the real values whilst *B* values are smaller due to the reduced thickness and hence the cross-section area of the flat part. In the case of overgrinding, one can take the sample out of the mount to measure the thickness after all the domain imaging are completed and then scale the *in situ* measured *B* values (for the sensor) by a factor equal to the designed/final thickness to approximate the real *B* values (for the sample), only as a remedy measure.

The activity of the ferro-fluid is particularly important to dynamic domain imaging. If the degree of DW movements falls short of expectation one should check the ferro-fluid performance on a familiar sample using a DC applied field. If the issue remains, the ferro-fluid needs replacing. Fresh ferro-fluid is most active and it settles during storage. It is recommended to make a small amount of fresh ferro-fluid by dilution using original solvent for each experiment. The data on the activity of the ferro-fluid or the response time (to the change of the domain structure of the

sample under examination) are not available whilst the latter is believed to be in the range of microseconds according to the supplier (Rene V, 2016). The frequency at which the magnetic field is applied for dynamic domain imaging in this investigation was 1 Hz, which is also the optimum frequency for major *BH* loop measurement. The performance of the ferro-fluid at higher magnetization frequency is yet to be assessed.

Whilst the Bitter method is convenient and sensitive its resolution is relatively low (about 1 μm)¹¹. This limits the application of the method for static domain patterns to steels that show DWs separate by > 2 μm . However, it is still of value for dynamic domain imaging as the domain size increases under the action of the applied fields. The present test rig can only apply a field parallel with the sample surface for *in situ BH* measurements. To study the effect of crystallographic texture or the DW movement processes of grain-orientated steels one needs to consider the texture or grain orientation at the specimen sampling stage to ensure an appropriate sample orientation is chosen.

The significance of the *in situ BH* loop measurement is twofold. First, it enables quantitative interpretation of DW movement processes in terms of the applied field and magnetic properties. Second, it helps establish a fundamental link between *BH* loop behaviors, magnetic properties and the microstructures of steels and ultimately helps interpreting EM sensor signals for microstructure evaluation. It is still challenging and of great significance to link the DW movement processes and/or domain structure to complex microstructures, particularly grain crystallographic orientations. In the future, electron back scattered diffraction (EBSD) analysis of the samples will be carried out and mapped to the static and dynamic domain patterns. The results will help interpret the different types of domain patterns observed in different grains and the different domain wall movement processes associated with the grain orientations with respect to the applied field directions.

When implemented correctly the *BH* loop produced by this method should be close to that produced using a closed magnetic circuit ring sample, as Parts A and B form a closed magnetic circuit. However, if both parts are not fitted perfectly together, an air gap will be introduced into the magnetic circuit and the results will be distorted. This distortion will present itself as *BH* loop shearing; a well-known effect characterized by an increase in maximum *H*, a decrease in magnetic remanence and the loop appearing more 'diagonal'. It is advisable to use the *BH* loop measurement system to acquire a *BH* loop using the Part A prior to mounting to compare to the loops acquired during the test, thus magnetic coupling can be assessed and repeatability optimized.

We chose the dimensions of the Part A and Part B considering the following factors and requirements. The reason for the differences of the Part A and Part B has been explained in Step 2.1. The mounting process described in Step 2 primarily dictates the horizontal length (25 mm, see Figure 1) of the samples used for these tests. A large polished surface area, determined by the horizontal length and the depth (4 mm, Figure 1) is beneficial to optical microscopy as well as sample preparation. The thickness of the sample should be the minimum required to produce a sufficiently rigid sample from the material under inspection; 1.5 mm in this case. The practicality

and cost of machining should also be considered when choosing the thickness. The smaller the transverse cross section of the sample, the greater the flux density that can be generated by the excitation coils for a given current. Higher currents lead to more heat being generated and the ferro-fluid quickly drying out. A large number of turns of the excitation coils is desirable. The length of the two legs (15 mm, Figure 1) dictates the height of the rig. The latter must be smaller than the maximum spacing between the sample stage and the objective lens of the microscope. The maximum flux density and applied field are best decided by the user and are application specific. It is clear from observation when the *BH* loop is close to saturation (the *BH* loop exhibits a very small dB/dH), but this section of the curve stretches from very low applied fields to very high applied fields and could require values approaching 100 kA/m before the material could truly be said to be magnetically saturated. From our experience maximum applied field of 2 kA/m (for pure iron or soft steels e.g. all the steels studied in this paper) – 10 kA/m (for hard steels e.g. a martensitic steel) should magnetize the sample beyond the ‘knee’ of its major *BH* loop, during which most significant domain wall movements are expected to occur.

In summary, the present system for domain imaging with *in situ BH* measurement proved to be working for linking the DW movement processes directly to the *BH* loop of steels. This method is anticipated to become a useful tool for the fundamental study of microstructure–magnetic property relationships in steels, in conjunction with further microstructural characterization.

ACKNOWLEDGMENTS:

The work was carried out with financial support from EPSRC under Grant EP/K027956/2. All the underlying data behind this article can be accessed from the corresponding author.

DISCLOSURES:

The authors have nothing to disclose.

REFERENCES:

- 1 Meilland, P., Kroos, J., Buchholtz, O. W. & Hartmann, H. J. Recent Developments in On-Line Assessment of Steel Strip Properties. *AIP Conf. Pro.* **820** (1), 1780-1785 (2006).
- 2 Davis, C. L., Dickinson, S. J. & Peyton, A. J. Impedance spectroscopy for remote analysis of steel microstructures. *Ironmak. Steelmak.* **32** 381-384, doi:10.1179/174328105x71254 (2005).
- 3 Dodd, C. V. & Deeds, W. E. Analytical Solutions to Eddy-Current Probe-Coil Problems. *J. Appl. Phys.* **39** (6), 2829-2838, doi:10.1063/1.1656680 (1968).
- 4 Liu, J., Wilson, J., Strangwood, M., Davis, C. L. & Peyton, A. Magnetic characterisation of microstructural feature distribution in P9 and T22 steels by major and minor *BH* loop measurements. *J. Magn. Magn. Mater.* **401** (1), 579-592, doi:10.1016/j.jmmm.2015.10.075 (2016).
- 5 Jiles, D. *Introduction to magnetism and magnetic materials*. 2nd edn, 171-175 (Chapman and Hall, 1998).
- 6 Liu, J., Wilson, J., Davis, C. & Peyton, A. in *55th Annual British Conference of Non-Destructive Testing* (Nottingham, UK, 2016).
- 7 Turner, S., Moses, A., Hall, J. & Jenkins, K. The effect of precipitate size on magnetic domain behavior in grain-oriented electrical steels. *J. Appl. Phys.* **107** (9), -,

522 doi:10.1063/1.3334201 (2010).

523 8 Chen, Z. J. & Jiles, D. C. Modelling of reversible domain wall motion under the action of
524 magnetic field and localized defects. *IEEE. T. Magn.* **29** (6), 2554-2556 (1993).

525 9 Takahashi, S., Kobayashi, S., Kikuchi, H. & Kamada, Y. Relationship between mechanical
526 and magnetic properties in cold rolled low carbon steel. *J. Appl. Phys.* **100** (11), 113908-113906,
527 doi:10.1063/1.2401048 (2006).

528 10 Kobayashi, S. *et al.* Changes of magnetic minor hysteresis loops during creep in Cr-Mo-V
529 ferritic steel. *J. Electr. Eng.* **59** (7s), 29-32 (2008).

530 11 Moses, A. J., Williams, P. I. & Hoshtanar, O. A. Real time dynamic domain observation in
531 bulk materials. *J. Magn. Magn. Mater.* **304** (2), 150-154, doi:10.1016/j.jmmm.2006.02.117
532 (2006).

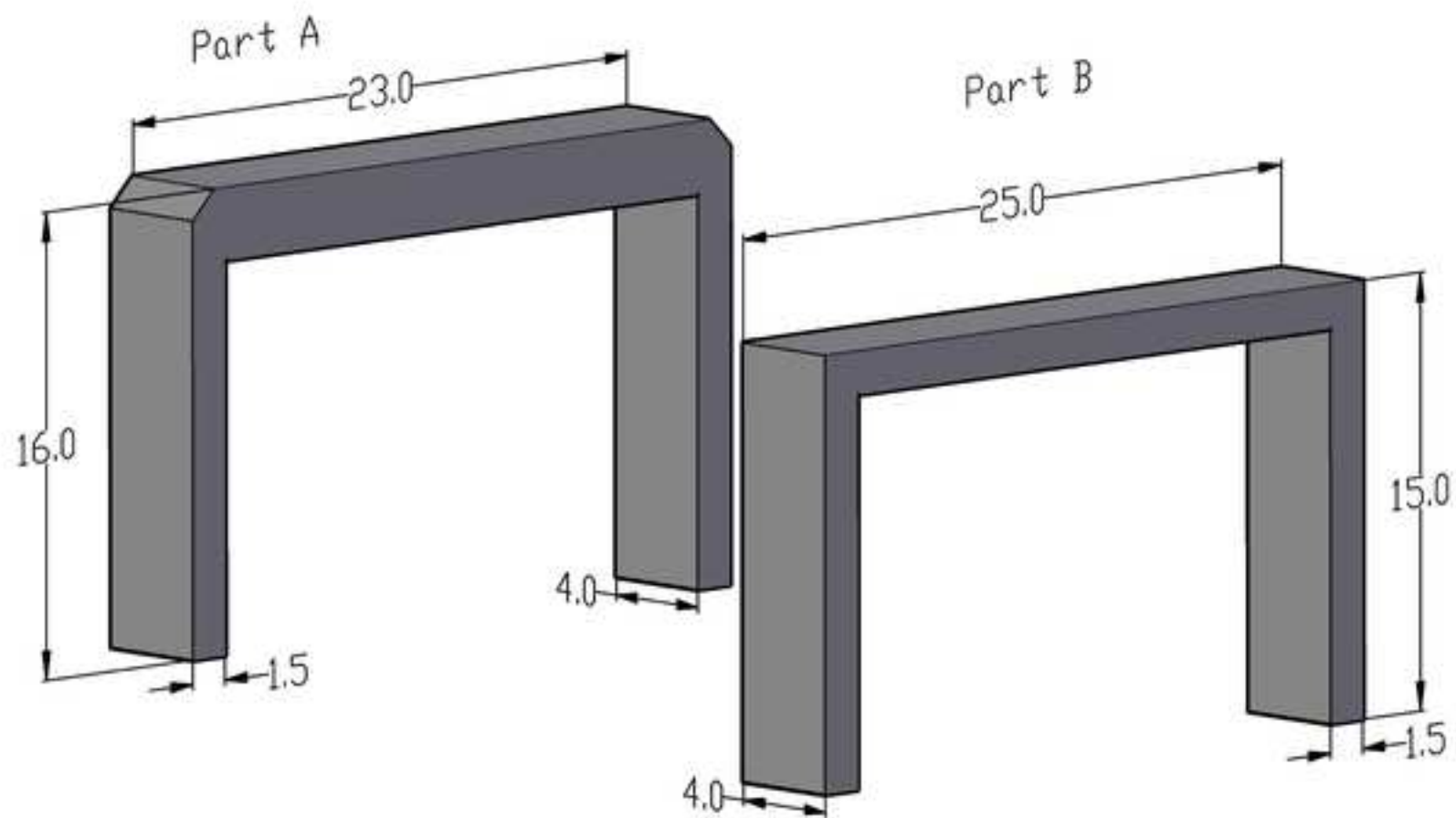
533 12 Williams, H. J., Bozorth, R. M. & Shockley, W. Magnetic Domain Patterns on Single Crystals
534 of Silicon Iron. *Physical Review.* **75** (1), 155-178, doi:10.1103/PhysRev.75.155 (1949).

535 13 Hubert, A. & Schäfer, R. in *Magnetic Domains: The Analysis of Magnetic Microstructures*
536 373-492 (Springer Berlin Heidelberg, 1998).

537 14 Buehler. *Buehler SumMet A Guide to Materials Preparation & Analysis*. 2nd edn, (Buehler,
538 2011).

539 15 Wilson, J. W. *et al.* Measurement of the magnetic properties of P9 and T22 steel taken
540 from service in power station. *J. Magn. Magn. Mater.* **360** (0), 52-58,
541 doi:10.1016/j.jmmm.2014.01.057 (2014).

542



Unit: mm

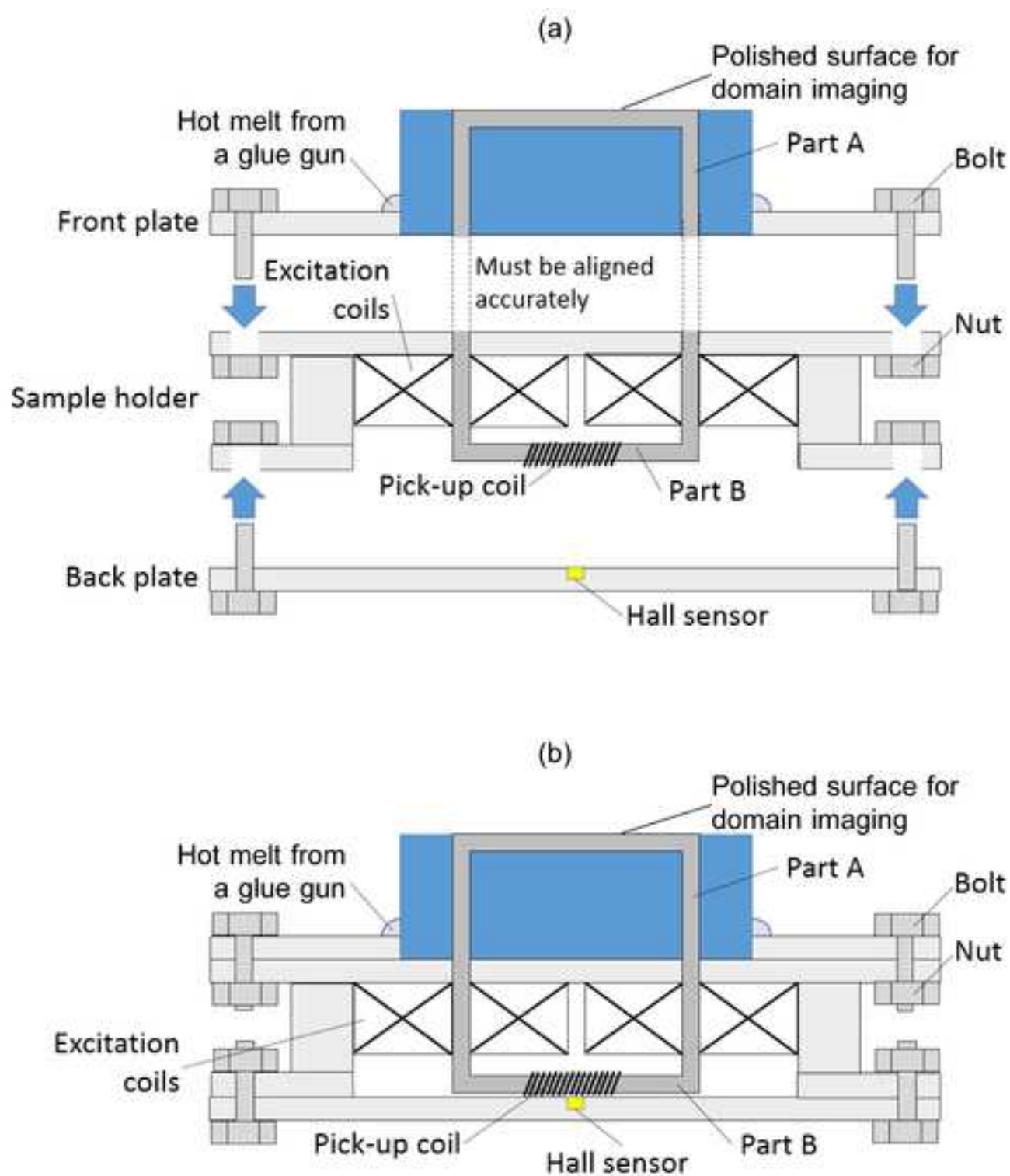


Figure 3

[Click here to download Figure Figure 3.jpg](#)

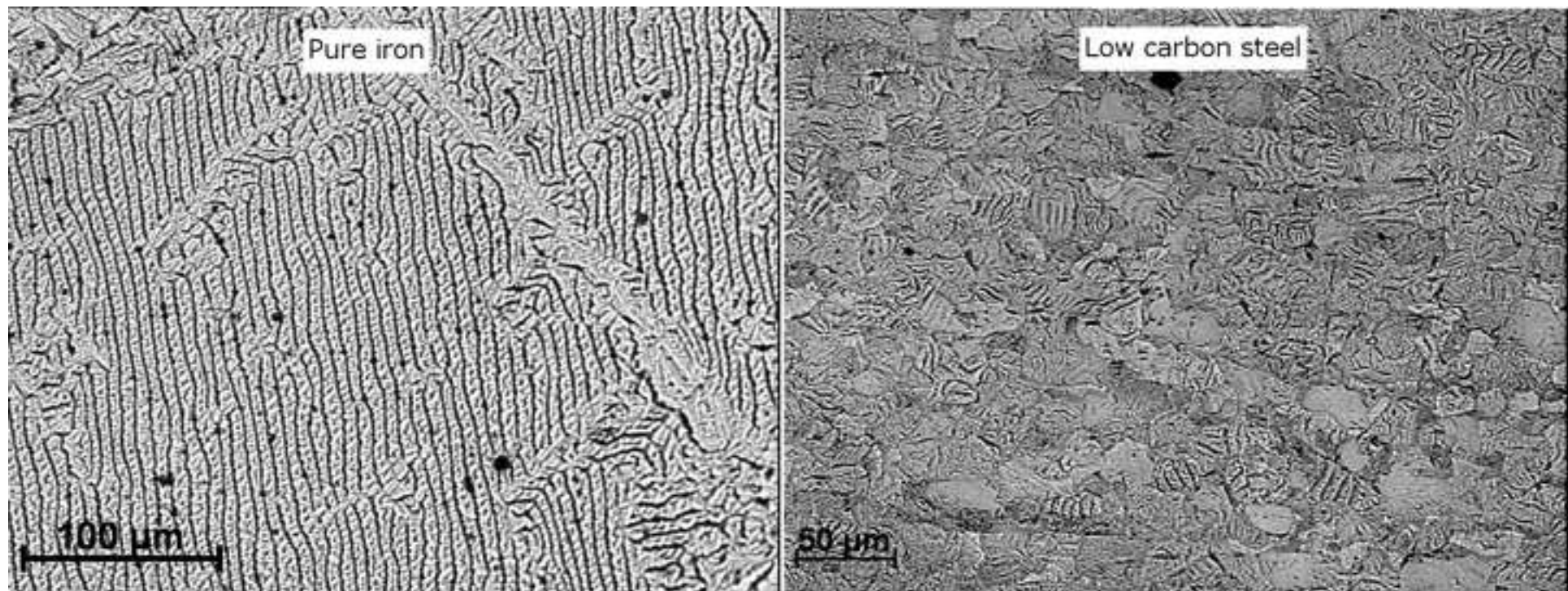


Figure 4

[Click here to download Figure figure 4.jpg](#)

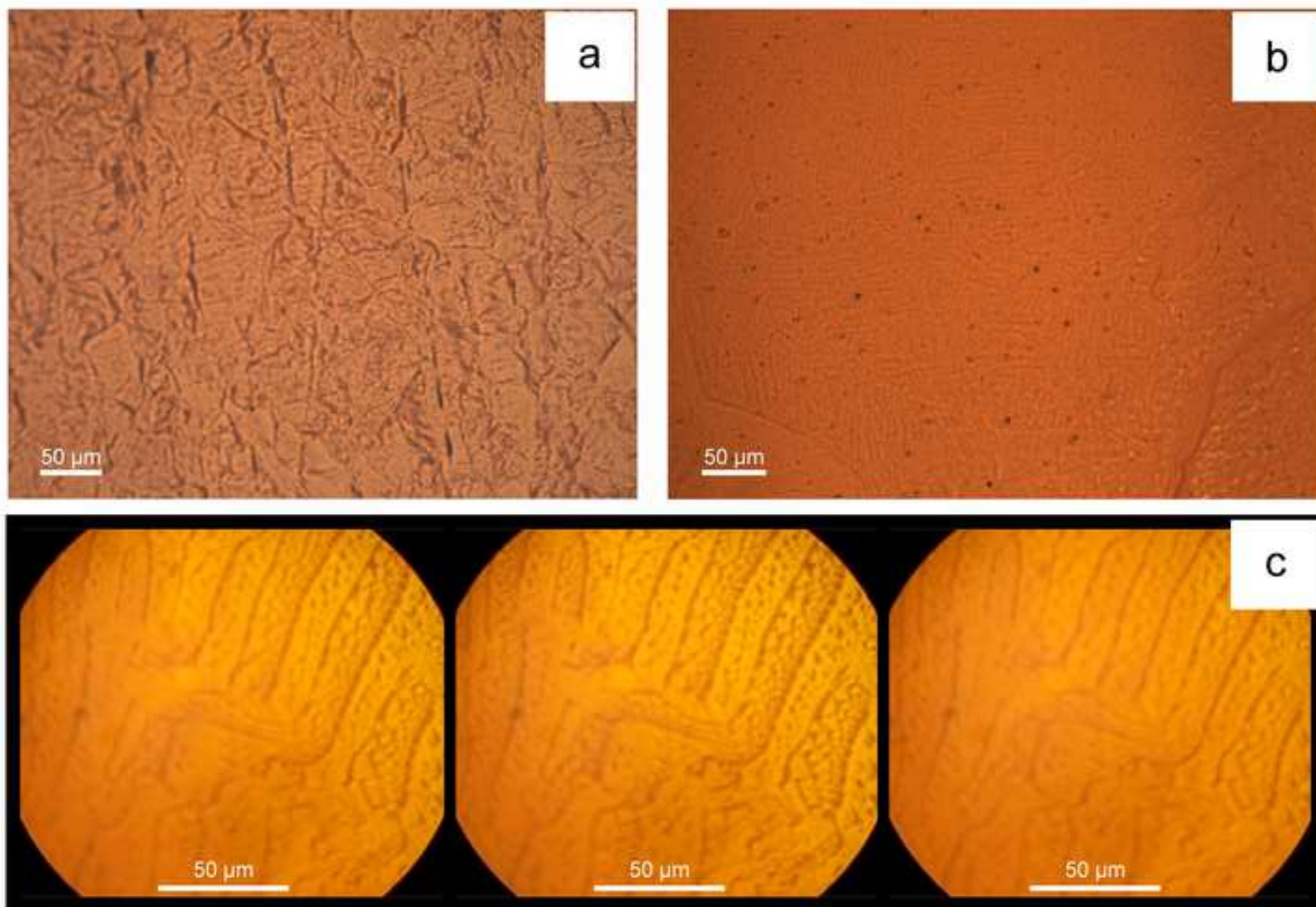
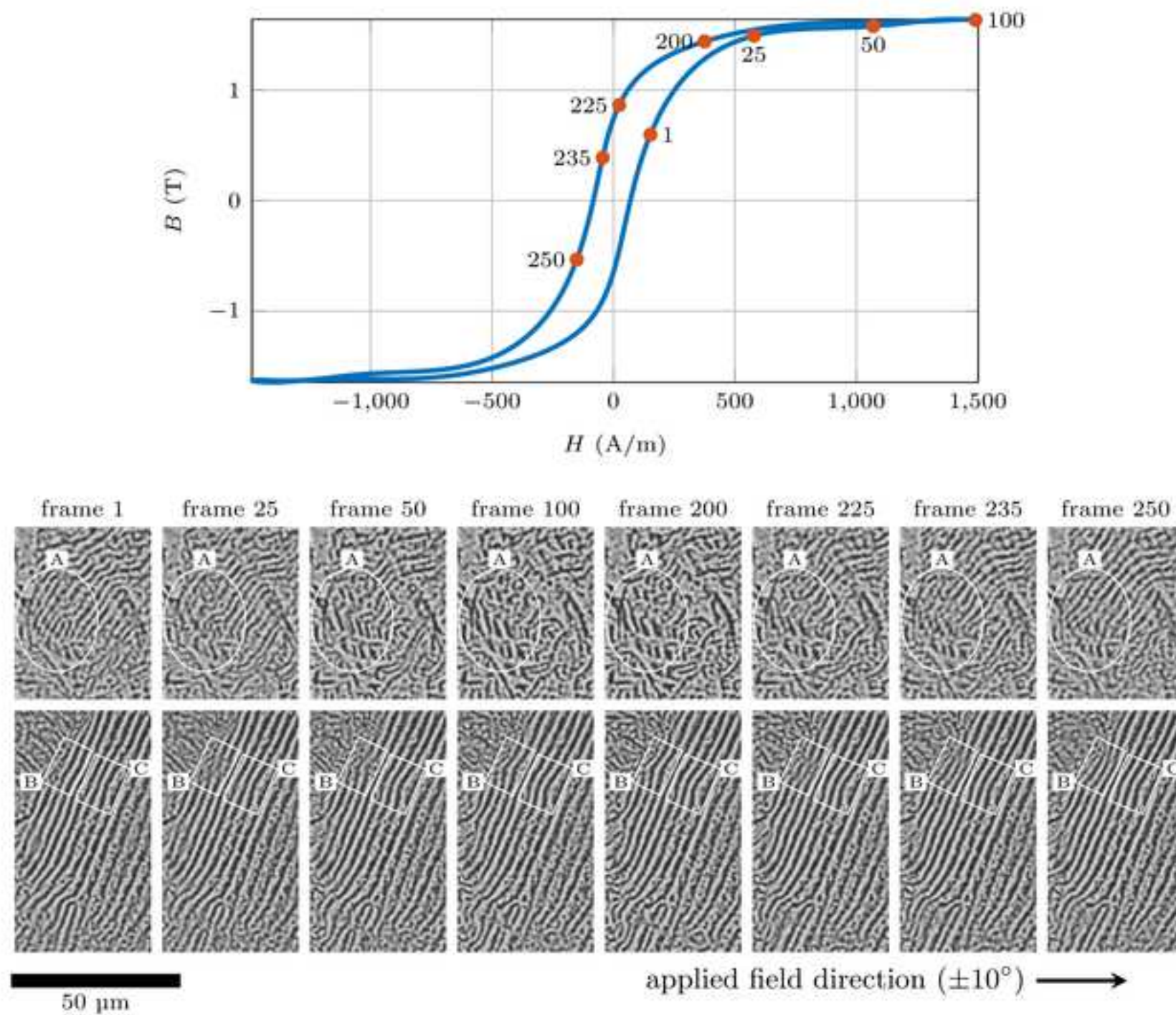


Figure 5

[Click here to download Figure figure 5.jpg](#)



Material and Equipment

Name of Material/ Equipment	Company	Catalog Number	Comments/Description
EMG 911 ferro-fluid	Ferrotec	89U1000000	Oil based Ferro-fluid for domain imaging
Solvent for EMG 900 series ferro-fluid	Ferrotec	89Z5000000	Original solvent for the EMG 900 series ferro-fluid for diluting the original ferro-fluid
AxioScope polarised light microscope	Zeiss AOS Technologies	430035-9270-000	
S-Mize High Speed Camera	AG	160021-10	High speed camera that can be connected to the microscope for recording videos
Midas DA Software	Xcitex, Inc		Synchronize the high-speed video with the <i>BH</i> data
MiDas DA Module BNC Breakout Box	Xcitex, Inc	185124H-01L	The hardware for data synchronizing the video and <i>BH</i> data
TransOptic mounting compounds	Buehler	20-3400-08	Transparent thermoplastic acrylic mounting material
MetaDi Supreme 9um diamond suspension	Buehler	406633128	9 µm diamond polishing suspension
MetaDi Supreme 3um diamond suspension	Buehler	406631128	3 µm diamond polishing suspension
MetaDi Supreme 1um diamond suspension	Buehler	406630032	1 µm diamond polishing suspension
MasterPrep polishing suspension	Buehler	406377032	Alumina polishing suspension
UltraPad polishing cloth	Buehler	407122	For 9 µm diamond polishing
TriDent polishing cloth	Buehler	407522	For 3 µm diamond polishing
ChemoMet polishing cloth	Buehler	407922	For 1 µm diamond polishing
MicroCloth polishing cloth	Buehler	407222	Final polishing using the alumina polishing suspension

Material and Equipment

Nital 2%	VWR International University of Manchester	DIUKNI4307A	For etching
<i>BH</i> analyzer		Not applicable	An in-house system for <i>BH</i> analysis

Title of Article:

Author(s):

Item 1 (check one box): The Author elects to have the Materials be made available (as described at

<http://www.jove.com/author>) via: ☐ Standard Access ☒ Open Access

Item 2 (check one box):

- ☒ The Author is NOT a United States government employee.
- ☐ The Author is a United States government employee and the Materials were prepared in the course of his or her duties as a United States government employee.
- ☐ The Author is a United States government employee but the Materials were NOT prepared in the course of his or her duties as a United States government employee.

ARTICLE AND VIDEO LICENSE AGREEMENT

1. **Defined Terms.** As used in this Article and Video License Agreement, the following terms shall have the following meanings: **"Agreement"** means this Article and Video License Agreement; **"Article"** means the article specified on the last page of this Agreement, including any associated materials such as texts, figures, tables, artwork, abstracts, or summaries contained therein; **"Author"** means the author who is a signatory to this Agreement; **"Collective Work"** means a work, such as a periodical issue, anthology or encyclopedia, in which the Materials in their entirety in unmodified form, along with a number of other contributions, constituting separate and independent works in themselves, are assembled into a collective whole; **"CRC License"** means the Creative Commons

Attribution 3.0 Agreement (also known as CC-BY), the terms and conditions of which can be found at: <http://creativecommons.org/licenses/by/3.0/us/legalcode>;

"Derivative Work" means a work based upon the Materials or upon the Materials and other pre-existing works, such as a translation, musical arrangement, dramatization, fictionalization, motion picture version, sound recording, art reproduction, abridgment, condensation, or any other form in which the Materials may be recast, transformed, or adapted; **"Institution"** means the institution, listed on the last page of this Agreement, by which the Author was employed at the time of the creation of the Materials; **"JoVE"** means MyJoVE Corporation, a Massachusetts corporation and the publisher of *The Journal of Visualized Experiments*;

"Materials" means the Article and / or the Video; **"Parties"** means the Author and JoVE; **"Video"** means any video(s) made by the Author, alone or in conjunction with any other parties, or by JoVE or its affiliates or agents, individually or in collaboration with the Author or any other parties, incorporating all or any portion of the Article, and in which the Author may or may not appear.

2. **Background.** The Author, who is the author of the Article, in order to ensure the dissemination and protection of the Article, desires to have the JoVE publish the Article and create and transmit videos based on the Article. In furtherance of such goals, the Parties desire to memorialize in this Agreement the respective rights of each Party in and to the Article and the Video.

3. **Grant of Rights in Article.** In consideration of JoVE agreeing to publish the Article, the Author hereby grants to JoVE, subject to **Sections 4 and 7** below, the exclusive, royalty-free, perpetual (for the full term of copyright in the Article, including any extensions thereto) license (a) to publish, reproduce, distribute, display and store the Article in all forms, formats and media whether now known or hereafter developed (including without limitation in print, digital and electronic form) throughout the world, (b) to translate the Article into other languages, create adaptations, summaries or extracts of the Article or other Derivative Works (including, without limitation, the Video) or Collective Works based on all or any portion of the Article and exercise all of the rights set forth in (a) above in such translations, adaptations, summaries, extracts, Derivative Works or Collective Works and

(c) to license others to do any or all of the above. The foregoing rights may be exercised in all media and formats, whether now known or hereafter devised, and include the right to make such modifications as are technically necessary to exercise the rights in other media and formats. If the "Open Access" box has been checked in **Item 1** above, JoVE and the Author hereby grant to the public all such rights in the Article as provided in, but subject to all limitations and requirements set forth in, the CRC License.

4. **Retention of Rights in Article.** Notwithstanding the exclusive license granted to JoVE in **Section 3** above, the

Author shall, with respect to the Article, retain the non-exclusive right to use all or part of the Article for the non-commercial purpose of giving lectures, presentations or teaching classes, and to post a copy of the Article on the

Institution's website or the Author's personal website, in each case provided that a link to the Article on the JoVE website is provided and notice of JoVE's copyright in the Article is included. All non-copyright intellectual property rights in and to the Article, such as patent rights, shall remain with the Author.

5. Grant of Rights in Video – Standard Access. This **Section 5** applies if the "Standard Access" box has been checked in **Item 1** above or if no box has been checked in **Item 1** above. In consideration of JoVE agreeing to produce, display or otherwise assist with the Video, the Author hereby acknowledges and agrees that, Subject to **Section 7** below, JoVE is and shall be the sole and exclusive owner of all rights of any nature, including, without limitation, all copyrights, in and to the Video. To the extent that, by law, the Author is deemed, now or at any time in the future, to have any rights of any nature in or to the Video, the Author hereby disclaims all such rights and transfers all such rights to JoVE.

6. Grant of Rights in Video – Open Access. This **Section 6** applies only if the "Open Access" box has been checked in **Item 1** above. In consideration of JoVE agreeing to produce, display or otherwise assist with the Video, the Author hereby grants to JoVE, subject to **Section 7** below, the exclusive, royalty-free, perpetual (for the full term of copyright in the Article, including any extensions thereto) license (a) to publish, reproduce, distribute, display and store the Video in all forms, formats and media whether now known or hereafter developed (including without limitation in print, digital and electronic form) throughout the world, (b) to translate the Video into other languages, create adaptations, summaries or extracts of the Video or other Derivative Works or Collective Works based on all or any portion of the Video and exercise all of the rights set forth in (a) above in such translations, adaptations, summaries, extracts, Derivative Works or Collective Works and (c) to license others to do any or all of the above. The foregoing rights may be exercised in all media and formats, whether now known or hereafter devised, and include the right to make such modifications as are technically necessary to exercise the rights in other media and formats.

7. Government Employees. If the Author is a United States government employee and the Article was prepared in the course of his or her duties as a United States government employee, as indicated in **Item 2** above, and any of the licenses or grants granted by the Author hereunder exceed the scope of the 17 U.S.C. 403, then the rights granted hereunder shall be limited to the maximum rights permitted under such statute. In such case, all provisions contained herein that are not in conflict with such statute shall remain in full force and effect, and all provisions contained herein that do so conflict

shall be deemed to be amended so as to provide to JoVE the maximum rights permissible within such statute.

8. Likeness, Privacy, Personality. The Author hereby grants JoVE the right to use the Author's name, voice, likeness, picture, photograph, image, biography and performance in any way, commercial or otherwise, in connection with the Materials and the sale, promotion and distribution thereof. The Author hereby waives any and all rights he or she may have, relating to his or her appearance in the Video or otherwise relating to the Materials, under all applicable privacy, likeness, personality or similar laws.

9. Author Warranties. The Author represents and warrants that the Article is original, that it has not been published, that the copyright interest is owned by the Author (or, if more than one author is listed at the beginning of this Agreement, by such authors collectively) and has not been assigned, licensed, or otherwise transferred to any other party. The Author represents and warrants that the author(s) listed at the top of this Agreement are the only authors of the Materials. If more than one author is listed at the top of this Agreement and if any such author has not entered into a separate Article and Video License Agreement with JoVE relating to the Materials, the Author represents and warrants that the Author has been authorized by each of the other such authors to execute this Agreement on his or her behalf and to bind him or her with respect to the terms of this Agreement as if each of them had been a party hereto as an Author. The Author warrants that the use, reproduction, distribution, public or private performance or display, and/or modification of all or any portion of the Materials does not and will not violate, infringe and/or misappropriate the patent, trademark, intellectual property or other rights of any third party. The Author represents and warrants that it has and will continue to comply with all government, institutional and other regulations, including, without limitation all institutional, laboratory, hospital, ethical, human and animal treatment, privacy, and all other rules, regulations, laws, procedures or guidelines, applicable to the Materials, and that all research involving human and animal subjects has been approved by the Author's relevant institutional review board.

10. JoVE Discretion. If the Author requests the assistance of JoVE in producing the Video in the Author's facility, the Author shall ensure that the presence of JoVE employees, agents or independent contractors is in accordance with the relevant regulations of the Author's institution. If more than one author is listed at the beginning of this Agreement, JoVE may, in its sole discretion, elect not take any action with respect to the Article until such time as it has received complete, executed Article and Video License Agreements from each such author. JoVE reserves the right, in its absolute and sole discretion and without giving any reason therefore, to accept or decline any work submitted to JoVE. JoVE and its employees, agents and independent contractors shall have full, unfettered access to the facilities of the Author or of the Author's institution as necessary to make the Video, whether actually published or not. JoVE has sole discretion as to the method of making and publishing the Materials, including,

without limitation, to all decisions regarding editing, lighting, filming, timing of publication, if any, length, quality, content and the like.

11. **Indemnification.** The Author agrees to indemnify JoVE and/or its successors and assigns from and against any and all claims, costs, and expenses, including attorney's fees, arising out of any breach of any warranty or other representations contained herein. The Author further agrees to indemnify and hold harmless JoVE from and against any and all claims, costs, and expenses, including attorney's fees, resulting from the breach by the Author of any representation or warranty contained herein or from allegations or instances of violation of intellectual property rights, damage to the Author's or the Author's institution's facilities, fraud, libel, defamation, research, equipment, experiments, property damage, personal injury, violations of institutional, laboratory, hospital, ethical, human and animal treatment, privacy or other rules, regulations, laws, procedures or guidelines, liabilities and other losses or damages related in any way to the submission of work to JoVE, making of videos by JoVE, or publication in JoVE or elsewhere by JoVE. The Author shall be responsible for, and shall hold JoVE harmless from, damages caused by lack of sterilization, lack of cleanliness or by contamination due to the making of a video by JoVE its employees, agents or independent contractors. All sterilization, cleanliness or decontamination procedures shall be solely the responsibility of the Author and shall be undertaken at the Author's expense. All indemnifications provided herein shall include JoVE's attorney's fees and costs related to said losses or


damages. Such indemnification and holding harmless shall include such losses or damages incurred by, or in connection with, acts or omissions of JoVE, its employees, agents or independent contractors.

12. **Fees.** To cover the cost incurred for publication, JoVE must receive payment before production and publication the Materials. Payment is due in 21 days of invoice. Should the Materials not be published due to an editorial or production decision, these funds will be returned to the Author. Withdrawal by the Author of any submitted Materials after final peer review approval will result in a US\$1,200 fee to cover pre-production expenses incurred by JoVE. If payment is not received by the completion of filming, production and publication of the Materials will be suspended until payment is received.

13. **Transfer, Governing Law.** This Agreement may be assigned by JoVE and shall inure to the benefits of any of JoVE's successors and assignees. This Agreement shall be governed and construed by the internal laws of the Commonwealth of Massachusetts without giving effect to any conflict of law provision thereunder. This Agreement may be executed in counterparts, each of which shall be deemed an original, but all of which together shall be deemed to me one and the same agreement. A signed copy of this Agreement delivered by facsimile, e-mail or other means of electronic transmission shall be deemed to have the same legal effect as delivery of an original signed copy of this Agreement.

A signed copy of this document must be sent with all new submissions. Only one Agreement required per submission.

AUTHOR:

Name:	Jun Liu	
Department:	WMG	
Institution:	University of Warwick	
Article Title:	Magnetic Domain Imaging with In-situ Hysteresis Measurement	
Signature:		Date: 6/4/2017

Please submit a signed and dated copy of this license by one of the following three methods:

- 1) Upload a scanned copy as a PDF to the JoVE submission site upon manuscript submission (preferred);
- 2) Fax the document to +1.866.381.2236; or
- 3) Mail the document to JoVE / Atn: JoVE Editorial / 1 Alewife Center Suite 200 / Cambridge, MA 02140

For questions, please email editorial@jove.com or call +1.617.945.9051.

MS # (internal use):

EDITORIAL COMMENTS:

1. Please revise the highlighting of the manuscript to be 2.75 pages or less. Currently, there are about 4 pages of highlighted protocol text. Please note that the 2.75 page limit is a haerd production limit to ensure that the videography can occur in a single day.

The length of the highlighted text has been reduced to be about 2.5 pages.

2. Some additional details are required in the protocol:
5.4.2: What magnetic field strength is used? Please provide specifics so we can film.
The detail is given in the text now.